

Battery Management System Development for Electric Vehicles and Fast Charging Infrastructure Improvement

Yu Yang, PhD

Hen-Geul Yeh, PhD

Cesar Ortiz



MINETA TRANSPORTATION INSTITUTE

Founded in 1991, the Mineta Transportation Institute (MTI), an organized research and training unit in partnership with the Lucas College and Graduate School of Business at San José State University (SJSU), increases mobility for all by improving the safety, efficiency, accessibility, and convenience of our nation's transportation system. Through research, education, workforce development, and technology transfer, we help create a connected world. MTI leads the [Mineta Consortium for Transportation Mobility \(MCTM\)](#) and the [Mineta Consortium for Equitable, Efficient, and Sustainable Transportation \(MCEEST\)](#) funded by the U.S. Department of Transportation, the [California State University Transportation Consortium \(CSUTC\)](#) funded by the State of California through Senate Bill I and the Climate Change and Extreme Events Training and Research (CCEETR) Program funded by the Federal Railroad Administration. MTI focuses on three primary responsibilities:

Research

MTI conducts multi-disciplinary research focused on surface transportation that contributes to effective decision making. Research areas include: active transportation; planning and policy; security and counterterrorism; sustainable transportation and land use; transit and passenger rail; transportation engineering; transportation finance; transportation technology; and workforce and labor. MTI research publications undergo expert peer review to ensure the quality of the research.

Education and Workforce Development

To ensure the efficient movement of people and products, we must prepare a new cohort of transportation professionals who are ready to lead a more diverse, inclusive, and equitable transportation industry. To help achieve this, MTI sponsors a suite of workforce development and education opportunities. The Institute supports educational programs offered by the Lucas Graduate School of Business: a Master of Science in Transportation Management, plus graduate certificates that include High-Speed and Intercity Rail Management and Transportation Security Management. These flexible programs offer live online classes so that working transportation professionals can pursue an advanced degree regardless of their location.

Information and Technology Transfer

MTI utilizes a diverse array of dissemination methods and media to ensure research results reach those responsible for managing change. These methods include publication, seminars, workshops, websites, social media, webinars, and other technology transfer mechanisms. Additionally, MTI promotes the availability of completed research to professional organizations and works to integrate the research findings into the graduate education program. MTI's extensive collection of transportation-related publications is integrated into San José State University's world-class Martin Luther King, Jr. Library.

Disclaimer

The contents of this report reflect the views of the authors, who are responsible for the facts and accuracy of the information presented herein. This document is disseminated in the interest of information exchange. MTI's research is funded, partially or entirely, by grants from the U.S. Department of Transportation, the U.S. Department of Homeland Security, the California Department of Transportation, and the California State University Office of the Chancellor, whom assume no liability for the contents or use thereof. This report does not constitute a standard specification, design standard, or regulation.

Report 24-23

Battery Management System Development for Electric Vehicles and Fast Charging Infrastructure Improvement

Yu Yang, PhD

Hen-Geul Yeh, PhD

Cesar Ortiz

July 2024

A publication of the
Mineta Transportation Institute
Created by Congress in 1991

College of Business
San José State University
San José, CA 95192-0219

TECHNICAL REPORT DOCUMENTATION PAGE

1. Report No. 24-23	2. Government Accession No.	3. Recipient's Catalog No.	
4. Title and Subtitle Battery Management System Development for Electric Vehicles and Fast Charging Infrastructure Improvement		5. Report Date July 2024	
		6. Performing Organization Code	
7. Authors Yu Yang, PhD Hen-Geul Yeh, PhD Cesar Ortiz		8. Performing Organization Report CA-MTI-2325	
9. Performing Organization Name and Address Mineta Transportation Institute College of Business San José State University San José, CA 95192-0219		10. Work Unit No.	
		11. Contract or Grant No. ZSB12017-SJAUX	
12. Sponsoring Agency Name and Address State of California SB1 2017/2018 Trustees of the California State University Sponsored Programs Administration 401 Golden Shore, 5 th Floor Long Beach, CA 90802		13. Type of Report and Period Covered	
		14. Sponsoring Agency Code	
15. Supplemental Notes 10.31979/mti.2024.2325			
16. Abstract The electric vehicle (EV) has become increasingly popular due to its being zero-emission. However, a significant challenge faced by EV drivers is the range anxiety associated with battery usage. Addressing this concern, this project develops a more efficient battery management system (BMS) for electric vehicles based on a real-time, state-of-charge (SOC) estimation. The proposed study delivers three modules: (1) a new equivalent circuit model (ECM) for lithium-ion batteries, (2) a new SOC estimator based on the moving horizon method, and (3) an on-board FPGA implementation of the classical Coulomb counting method for SOC estimation. The research team extends the traditional ECM by incorporating more functional features through the least absolute shrinkage and selection operator (LASSO). Then the first-order transfer function model identification and LASSO are iteratively executed to minimize the data fitting error. Given this model, the research team employs the moving horizon estimator (MHE) to determine the SOC by fitting the measured terminal voltage. Subsequently, the research team implements the SOC estimation scheme on an FPGA board. This hardware-in-the-loop simulation is demonstrated in this report step by step. The proposed research has broad societal impacts. It aligns with SB1 objectives in several ways. First, EVs with a more efficient BMS can improve their cruise range, reducing energy consumption and traffic congestion. Second, the resulting BMS can be applied in the solar-power and battery-assisted charging stations to make more reliable infrastructure in an age of sustainable transportation.			
17. Key Words Electric vehicle charging, Lithium batteries, Estimation theory, Microprocessors, Vehicle range		18. Distribution Statement No restrictions. This document is available to the public through The National Technical Information Service, Springfield, VA 22161.	
19. Security Classif. (of this report) Unclassified	20. Security Classif. (of this page) Unclassified	21. No. of Pages 44	22. Price

Copyright © 2024

by **Mineta Transportation Institute**

All rights reserved.

DOI: 10.31979/mti.2024.2325

Mineta Transportation Institute
College of Business
San José State University
San José, CA 95192-0219

Tel: (408) 924-7560
Fax: (408) 924-7565
Email: mineta-institute@sjsu.edu

transweb.sjsu.edu/research/2325

ACKNOWLEDGMENTS

The authors are grateful to California State University, Long Beach (CSULB), College of Engineering. The authors also thank CSULB students Kyle Kuttler and Bryan Aguirre for their technical support. Finally, this project is financially supported by the Mineta Transportation Institute at San José State University.

CONTENTS

Acknowledgments.....	vi
List of Figures.....	viii
List of Tables	ix
Executive Summary	1
1. Introduction	2
1.1 Project Motivation and Background.....	2
1.2 Project Methods	5
2. Battery Modeling and SOC Estimation	7
2.1 Battery Modeling.....	7
2.2 SOC Estimation.....	11
2.3 Simulation Results.....	13
3. FPGA Implementation.....	19
3.1 Analysis of the Coulomb Counting Equation	19
3.2 Implementation on MATLAB/SIMULINK.....	19
3.3 FPGA-in-the-Loop Simulation	21
4. Summary & Conclusions	28
Glossary	29
Bibliography.....	31
About the Authors.....	34

LIST OF FIGURES

Figure 1. A Typical Structure and Functions of a Battery Management System	3
Figure 2. The BMS Architecture with FPGA Implementation	4
Figure 3. The Thevenin Equivalent Circuit Model	7
Figure 4. An Iterative Scheme for Battery Model Identification	10
Figure 5. The Battery Model Output vs. Measurement on Training Set	15
Figure 6. The Battery Model Output vs. Measurement on Validation Set.....	15
Figure 7. SOC Estimation Based on Coulomb Approaches.....	16
Figure 8. SOC Estimation Based on VC-MHE and V-MHE (Starting: 40500).....	17
Figure 9. SOC Estimation Based on VC-MHE and V-MHE (Starting: 99900).....	18
Figure 10. SIMULINK Build-in Function.....	20
Figure 11. SIMULINK SOC Subsystem with Convert Blocks.....	20
Figure 12. SIMULINK HDL Code Generation.....	21
Figure 13. Introduce Board Name: Basys3	22
Figure 14. FPGA-in-the-Loop Interface	23
Figure 15. FPGA-in-the-Loop (FIL Options)	24
Figure 16. FPGA-in-the-Loop (Source Files).....	25
Figure 17. FPGA-in-the-Loop (DUT I/O Ports).....	26
Figure 18. Reconstruct SOC Estimation Block with FIL	27
Figure 19. SOC Estimation Results via FIL.....	27

LIST OF TABLES

Table 1. MAE on Training Datasets in Each Iteration and Validation Set	14
Table 2. Battery Model Parameters	14
Table 3. Improved Coulomb Model Parameters	17
Table 4. SOC Estimation Results at Sampled Periods	17

Executive Summary

With the increasing adoption of electric vehicles (EVs) in the transportation sector, range anxiety has become pervasive among EV drivers. A poor lithium-ion battery used in EVs will reduce the rated cruise range, cause safety issues and worsen traffic congestion. To address these challenges without imposing additional costs on customers for battery replacement, the integration of an efficient Battery Management System (BMS) emerges as a viable solution to alleviate range anxiety and prolong battery lifespan. The core function of BMS is the state-of-charge (SOC) estimation to monitor the battery status and provide feedback information to the central control unit. In pursuit of enhanced BMS efficiency, the research team proposes a new equivalent circuit model (ECM) to the lithium-ion battery, an approach designed to identify its parameters. Leveraging this ECM, the research team estimates SOC from measured terminal voltage data using a voltage-and-current-based moving horizon estimator (VC-MHE). Compared with existing approaches, the advantage of the proposed method is that it does not need the SOC-OCV curve a priori and, thus, can be applied in any circumstances.

Our research methodology involves the collection and processing of an open-source test dataset for the commonly used Sanyo battery 18650 3.7V 2.6Ah. The software platform for battery modeling and VC-MHE is MATLAB with various state-of-the-art optimization solvers, such as SCIP and IPOPT, to ensure optimality in the moving horizon estimator (MHE). To enable hardware-in-the-loop simulation for practical BMS development, the research team implements a classical SOC algorithm on an FPGA board and provides a comprehensive guide for software and hardware setup.

The work yielded the following discoveries:

- New functional features can be introduced into the ECM and refined by the least absolute shrinkage and selection operator (LASSO) method to improve the data-driven model accuracy.
- The VC-MHE performs better than the voltage-based method for the battery status, such as SOC and estimation accuracy.
- The MATLAB/SIMULINK can convert the high-level software programming to the hardware description language (HDL) coding of FPGA, significantly reducing the development period.

This research not only provides new EV battery modeling techniques but also shows the potential of using FPGA to implement advanced algorithms for real time battery management.

1. Introduction

This project aims to develop a more efficient battery management system (BMS) for electric vehicles (EVs) and their charging infrastructure based on real-time monitoring, machine learning, and optimal control. The research team conducts algorithm development and hardware-in-the-loop simulation. It also trains students from the electrical and chemical engineering departments at California State University, Long Beach in battery energy storage for transportation applications.

The proposed project has significant potential for knowledge advancement. Our study will deliver three modules: (1) a new equivalent circuit model (ECM) for lithium-ion battery fast charging through feature selection, (2) a new state-of-charge (SOC) estimation algorithm, and (3) an on-board field-programmable gate array (FPGA) implementation of the SOC estimation. Our research will answer the following two questions: (1) how to integrate advanced optimization technology and empirical battery models to improve the SOC estimation and (2) how to develop an on-board FPGA platform for hardware-in-the-loop simulation. Compared with existing battery monitoring techniques, the proposed approaches establish a more efficient way to identify ECM and estimate SOC. Even though it is more computationally demanding, the FPGA can provide sufficient computational power for implementation.

The proposed research also has broad societal impacts. It aligns with SB1 objectives in a multifaceted manner. First, EVs with a more efficient BMS can improve their cruise range, and thus reduce energy consumption and traffic congestion. Second, the BMS algorithms resulting from this research can be applied in the solar power and battery-assisted charging stations to make infrastructure environmentally cleaner. Third, the developed system and software promises to be useful in the zero-emission vehicle (ZEV) workforce training. Finally, the SOC estimation algorithms will be deployed on a FPGA board using the MATLAB/SIMULINK platform, which enables industry-level management system development.

1.1 Project Motivation and Background

The Bipartisan Infrastructure Law, CHIPS & Science Act, and Inflation Reduction Act combined will spend more than \$135 billion to form the USA's electric vehicle future (White House, Oct 19, 2022). Within the state, the California government set an ambitious goal of 5 million ZEVS on the road by 2030, but only 862,874 cumulative ZEV sales were achieved through the first quarter of 2021 (Alexander et al., 2021). One of the barriers to EV adoption is the limitation of traveling range on one charge, which is highly reliant on the battery performance and its management strategy. The Department of Energy (DOE) thus recently awarded \$2.8 billion to the study of battery development and battery management systems. Because the battery conditions cannot be directly measured in real time, a BMS is necessary to estimate battery pack performance and control the charging/discharging rate for energy efficiency improvement and safety enhancement. It is worthwhile to note that the BMS is not only applicable for EVs, but it can also

be used in any energy storage infrastructures, such as solar-power-assisted charging stations. The integration of BMSs and infrastructure will promote more efficient and cleaner energy solutions within the transportation system. Even though many BMSs have been commercialized, the limitations of existing BMSs are still significant, including the following issues:

1. The cycle-adaptive model for lithium-ion battery is absent.
2. The big data-driven SOC estimation is still unsatisfactory due to the limitation of model structure.
3. The energy-effective control system for fast charging is not well-developed.

The proposed research project conducts the preliminary studies on the key technologies of BMS, including battery modeling, state estimation, and hardware implementation. A typical structure and function of a BMS are shown in Fig 1. Due to the project time limitation, cell balancing and thermal management are not discussed in this report.

Figure 1. A Typical Structure and Functions of a Battery Management System

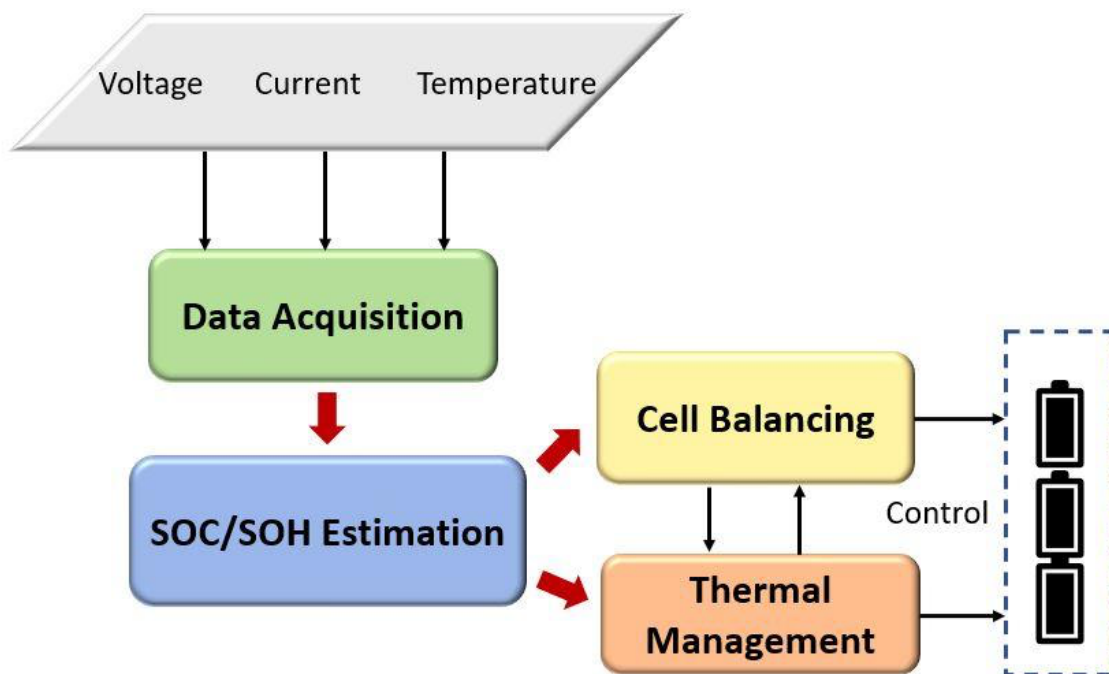
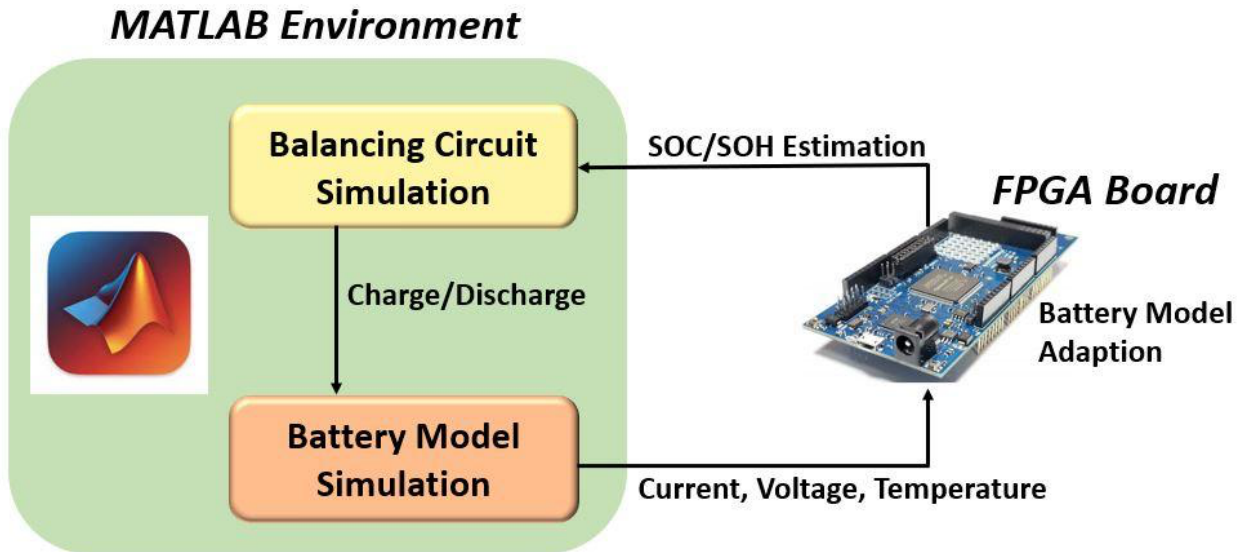


Figure 2. The BMS Architecture with FPGA Implementation



Battery Modeling

The traditional battery modeling approaches for SOC and SOH estimations can be categorized into two groups: (1) the equivalent circuit method (ECM) and (2) the electrochemical method. The ECM only needs to identify differential algebraic equations (DAEs) with 2-3 states and thus enjoys simplicity and fast execution. ECM mainly focuses on low-rate charging/discharging dynamics but may suffer from low prediction accuracy (Smith et al., 2007). Gandolfo et al. (2015) developed a one-resistor-based ECM for the SOC forecast of lithium polymer batteries. To improve the accuracy, the Thevenin ECM combining an internal ohmic resistance and a resistor-capacitor pair is widely used to represent the battery dynamics. The electrochemical method develops battery models using electrochemical theories. The resulting pseudo-two-dimensional (P2D) model is able to describe the battery dynamics under various operation conditions but may not be suitable for real-time computation. Hence, model reduction becomes a research hotspot. Dao et al. (2012) developed a simplified battery model using volume-average integration and Galerkin's approximation of the concentrated solution and the porous electrode theories. Smith et al. (2010) first proposed 4 PDEs based on the conservation law, coupled with the Butler-Volmer equation describing the reaction current at the solid/electrolyte interface. Then they reduced the model order by lumping modes with similar eigenvalues. Cai and White (2009) used the proper orthogonal decomposition (POD) to simplify the full-order physical model.

A new trend is to use machine learning for battery modeling. For example, Wang et al. (2017) proposed a thermal-electrical coupled model based on the neural network (NN) and validated its accuracy through battery tests. Dong et al. (2015) integrated the wavelet and NN to form a more complex data-driven model for the battery. Even though machine learning can accurately describe the nonlinear dynamics of a plant, its performance is highly dependent on the quality of the training dataset. For a time-varying system, such as a battery, making the model adaptive is still challenging.

SOC/SOH Estimation

Once the battery model structure is determined, the SOC and SOH estimations can be conducted. The SOC represents the capacity of a battery during a single charge/discharge cycle. The SOH represents the capacity deduction after a number of charging/discharging cycles. For safety, the EV battery cells have reached their end-of-life when the SOH is faded to 80% of its original rated capacity (Etxandi-Santolaya et al., 2024; Berecibar et al., 2016). The Coulomb counting method is one of the most popular methods because it is model-free, integrating the discharge current to estimate the SOC. An enhanced Coulomb counting method was proposed by considering the charging and operating efficiencies (Ng et al., 2009). The Kalman filter is commonly used for linear battery models (Yatsui & Bai, 2011; Smith et al., 2010). An adaptive unscented Kalman filtering (UKF) was applied in Sun et al. (2011) to estimate SOC based on the zero-state hysteresis battery model with a covariances adjustment. Furthermore, He et al. (2013) investigated the impact of temperature, charge-discharge rate, and running mileage on the SOC and applied the unscented particle filter (UPF) method to overcome the parameter perturbations. Machine learning can be used for SOC and SOH estimation, as mentioned above. For example, Sahinoglu et al. (2017) applied Gaussian Process (GP) regression to estimate the SOC of Li-ion batteries. The GP is suitable for small datasets and predicting intrinsic uncertainties of a safety-critical system, such as battery packs (Richardson et al., 2017). Yang et al. (2017) reported NN combined with the first-order ECM to predict the SOH.

On-board BMS

A MATLAB-to-FPGA design flow is applied in the proposed project because of its high performance, low cost, and agile development cycle. Kumar et al. (2018) have shown that neural network, fuzzy logic, and a statistical controller trained by MATLAB can be deployed to the FPGA board for SOC/SOH estimation. The hardware description language (HDL) codes describing the advanced BMS functions can be loaded to the FPGA using MATLAB's HDL Coder Toolbox. The battery model in MATLAB can generate the SOC data within seconds, rather than waiting for several hours of charging/discharging and can, thus, avoid any potential safety hazard. These data are transferred to FPGA for SOC/SOH estimation, and the control signal is sent back to MATLAB or real circuits for charging/discharging operations. This MATLAB-to-FPGA setting is suitable for the preliminary research without using any high-cost battery test system.

1.2 Project Methods

The project includes three specific aims. Aim one involves using open-source data to build a battery model. Aim two involves estimating the SOC through a current and voltage integrated approach. And aim three integrates a modular-based BMS on MATLAB and an FPGA board.

Aim One: Analyze the open-source charging/discharging datasets to build a machine learning and equivalent circuit hybrid model.

An open-source dataset is collected for battery modeling. The fast-charging data for Sanyo battery 18650 3.7V 2.6Ah is obtained from Gun et al. (2015) at the University of California Berkley under the CC BY 4.0 license. This dataset consists of voltage, current, and temperature of the battery under different c-rates of charging or discharging, which can be used for short-term dynamics modeling. Note that the 18650 battery is reliably and consistently used for most lithium-battery-modeling literature.

Given the data, the research team constructs the battery model in two steps. First, the static ECM parameters are identified through the open-source datasets using LASSO. In the second step, the dynamic component of ECM is modeled as a discrete transfer function. Different from other data-driven modeling schemes that focus on machine learning algorithms, our approach extracts and selects the crucial features for cycle-dependent and temperature-dependent dynamics. The input to any data-driven algorithm's features plays a crucial role in impacting the model performance. These features usually are problem-specific and should be designed carefully. The full voltage cycle data, current, number of cycles, and temperature can be used as raw data feeding into a feature-generation algorithm. The resulting feature candidates can be high-order polynomials and derivatives, or they can be constructed based on electrochemistry knowledge. Then a feature selection procedure is developed to determine a subset of features that can capture the cycle-varying and temperature-varying dynamics of the battery status.

Aim Two: Estimate SOC using the MATLAB-based optimization toolbox.

The proposed SOC estimation is based on a new Coulomb counting method (current-based) and MHE using the voltage-based ECM model. Because the ECM and Coulomb counting parameters are characterized through LASSO offline, the SOC calculation can be cast as an online model-based optimization problem over the estimation horizon. MHE aims to match the measured terminal voltage influenced by the SOC, internal resistance, and hysteresis (Plett, 2004) while weighting the SOC change calculated by the proposed new Coulomb counting model in the objective function.

Aim Three: Implement algorithms on the FPGA.

The proposed hardware-in-the-loop BMS platform has the architecture shown in Figure 2. The battery model and SOC estimation algorithm are designed, interacted, and simulated in MATLAB. The battery measurement data will be sent to the FPGA for on-board battery model and SOC algorithm implementation. Finally, the estimated SOC data from FPGA will flow back to Simulink for comparison.

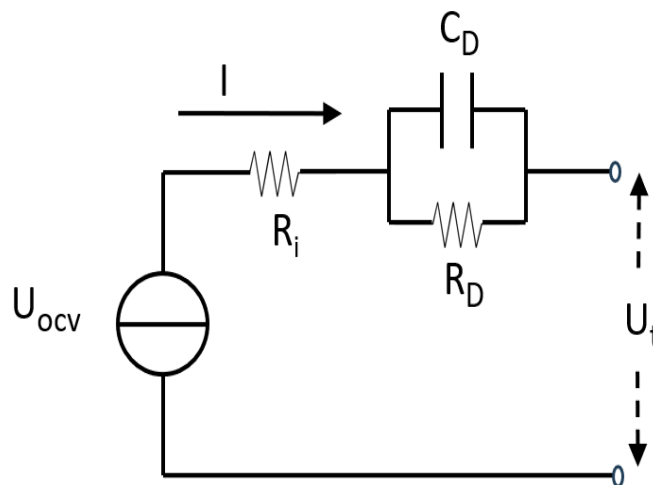
2. Battery Modeling and SOC Estimation

2.1 Battery Modeling

ECM uses Li-ion battery cells' characteristics with the combination of the use of resistors, capacitors, and voltage sources for modeling and can be applied to many different applications. In a paper for 18659 3.03Ah LiNiCoAlO₂ (NCA) battery modeling (Widanage et al. 2016), the results showed that the Root Mean Square Error (RMSE) and peak error (pk-error) of nonlinear methods compared to the linear method was improved by 13%-25% for RMSE and 52%- 62% for pk-error. It varies because that paper used four different temperatures: 10 °C, 15 °C, 25 °C, and 45 °C, under five different SOC percentages of the battery: 10%, 20% 50% 80%, and 95%. Liaw et al. (2004) presented a variation of the equivalent circuit model where all the ohmic resistant components lumped into resistor 1 and faradic non-linear components into the RC circuit. The battery used was 18650 cell and consisted of the following components: a MAG-10 graphite-negative electrode, a LiNi_{0.8}Co_{0.15}Al_{0.05}O₂-positive electrode, and 1.2 M LiPF₆ in ethyl carbonate/ethyl methyl carbonate (3:7 wt. % ratio). The paper stated that their current model, the behavior of the resistor with SOC, seems to be composed of at least two independent contributions. The contribution dominating in the higher SOC region follows a “power law,” whereas the “exponential law” dominates the lower SOC region.

In this subsection, a new ECM will be developed without knowing the OCV-SOC curve a priori. The conventional Thevenin ECM is plotted in Figure 3.

Figure 3. The Thevenin Equivalent Circuit Model



$$U_t(k) = U_{OCV}(k) - I(k)R_I - U_D(k), \quad (1)$$

$$U_D(k) = \exp\left(\frac{-\Delta t}{R_D C_D}\right) U_D(k-1) + R_D \left(1 - \exp\left(\frac{-\Delta t}{R_D C_D}\right)\right) I(k), \quad (2)$$

where $U_t(k)$ is the terminal voltage at time instant k ; U_D is the first-order diffusion voltage; I is the charging/discharging current; and U_{OCV} is the open-circuit voltage, which depends on the temperature and SOC while showing electro-chemical hysteresis. Here we temporarily omit the time index k and assume the non-diffusion voltage has the following structure:

when $I > 0$,

$$\begin{aligned} U_{OCV}(k) - I(k)R_I^{(+)} &= \alpha_0^{(+)} + \alpha_1^{(+)}s + \alpha_2^{(+)}\exp(-s) + \alpha_3^{(+)}\log(1-s) + \alpha_4^{(+)}\log(s) + \\ &\alpha_5^{(+)}\frac{1}{s} + \alpha_6^{(+)}T + \alpha_7^{(+)}\exp(-s)I + \alpha_8^{(+)}IT\exp(-s) + \alpha_9^{(+)}I\log(s) + \alpha_{10}^{(+)}s^2 + \\ &\alpha_{11}^{(+)}\frac{\exp\left(\frac{-\log(s)^2}{2}\right)}{s} + \alpha_{12}^{(+)}\frac{\exp\left(\frac{-\log(s)^2}{2}\right)}{T} + \alpha_{13}^{(+)}(s-0.5)^2, \end{aligned} \quad (3)$$

when $I \leq 0$,

$$\begin{aligned} U_{OCV}(k) - I(k)R_I^{(-)} &= \alpha_0^{(-)} + \alpha_1^{(-)}s + \alpha_2^{(-)}\exp(-s) + \alpha_3^{(+)}\log(1-s) + \alpha_4^{(+)}\log(s) + \\ &\alpha_5^{(+)}\frac{1}{s} + \alpha_6^{(+)}T + \alpha_7^{(+)}\exp(-s)I + \alpha_8^{(+)}IT\exp(-s) + \alpha_9^{(+)}I\log(s) + \alpha_{10}^{(+)}s^2 + \\ &\alpha_{11}^{(+)}\frac{\exp\left(\frac{-\log(s)^2}{2}\right)}{s} + \alpha_{12}^{(+)}\frac{\exp\left(\frac{-\log(s)^2}{2}\right)}{T} + \alpha_{13}^{(+)}(s-0.5)^2, \end{aligned} \quad (4)$$

where $\alpha_i^{(+)}$ and $\alpha_i^{(-)}$ are the model coefficient for discharging and charging, respectively; s represents the cell SOC; and T is the temperature.

Several points about these two equations are noteworthy. First, we identify the charging and discharging models of non-diffusion voltage separately owing to the electro-chemical hysteresis. Second, the terms associated with $\alpha_0, \alpha_1, \dots, \alpha_6$ are widely used for the OCV-SOC curve approximation in literature. However, our study shows that merely using these terms is not sufficient to approximate the voltage if the OCV-SOC curve is not known a priori. In fact, the OCV-SOC curve is temperature-dependent and can be impacted by the charging/discharging rate. Therefore, we integrate more functional features to enrich the representativeness of the model. Third, conventional OCV-SOC modeling methods rely on least squares to determine model parameters. Alternatively, the research team proposes using LASSO to identify model parameters while selecting functional features in Equations (3) and (4). By omitting the superscript (+) and (-), the formula of LASSO is the following:

$$\frac{1}{2|\Omega|} \left(\sum_{k \in \Omega} U_{OCV}(k) - I(k)R_I - f^T(k)\alpha \right) + \lambda \sum_{i=1}^{13} \alpha_i \quad (5)$$

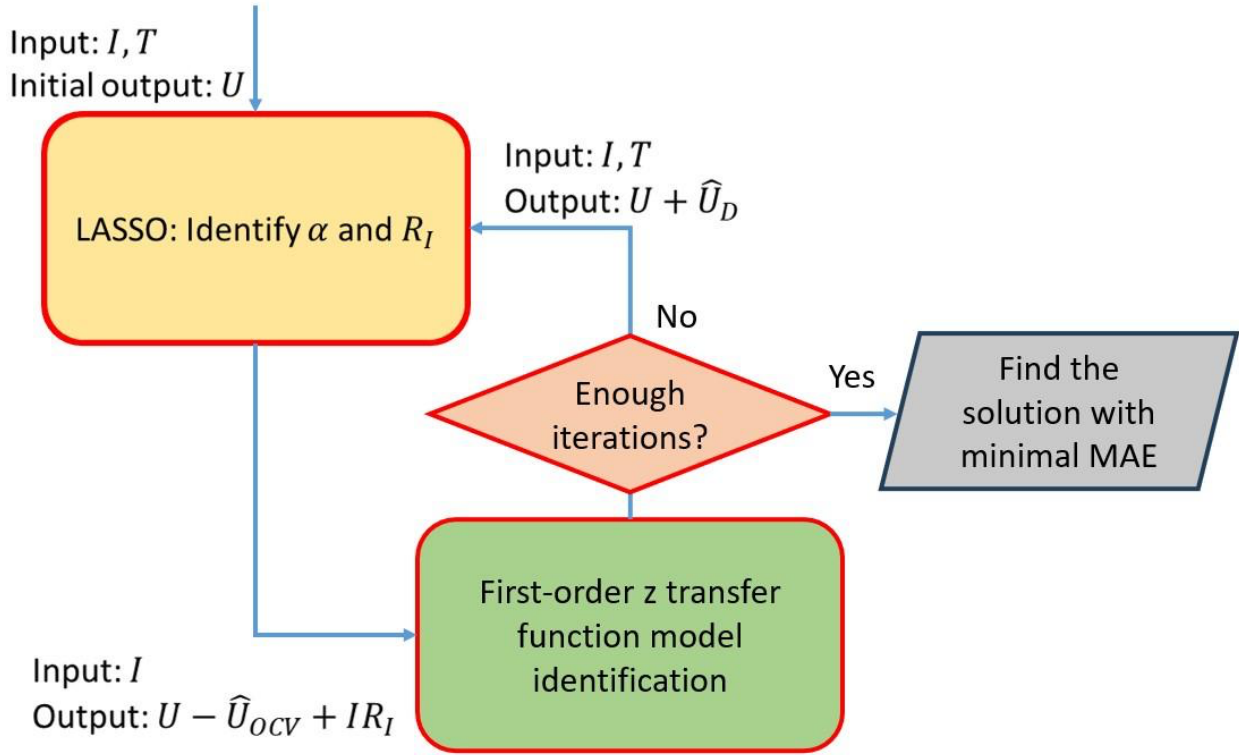
where Ω represents the charging or discharging dataset, $|\cdot|$ is the operator of cardinality, and f represents the feature vector associated with α in Eqs. (3) and (4).

$$f = \left[1; s(k); \exp(-s(k)); \log \log (1 - s(k)); \log \log (s(k)) ; \frac{1}{s(k)}; T(k); I \cdot \exp(-s(k)); I(k) \cdot T(k) \cdot \exp(-s(k)); I(k) \log \log (s(k)); s^2(k); \frac{\exp\left(-\frac{\log \log (s(k))^2}{2}\right)}{s(k)} ; \frac{\exp\left(-\frac{\log \log (s(k))^2}{2}\right)}{T(k)} ; (s(k) - 0.5)^2 \right] \quad (6)$$

λ is a non-negative regularization parameter that can be tuned by cross-validation through MATLAB's LASSO function. The working principle of LASSO is conducting both feature selection and regression simultaneously to achieve better prediction accuracy and reduce the chance of over-fitting. This is important because we do not know how these functional features impact the model performance before the data fitting. Some of the features contribute to the charging model but may be redundant to the discharging data fitting or vice versa. The LASSO provides a flexible framework for the analysis of any battery test datasets and enables integrating more features in future work.

Eq. (1) shows that the measurement $U_t(k)$ consists of two components: diffusion part $U_D(k)$ and non-diffusion U_{OCV} . LASSO can be applied in modeling U_{OCV} . Eq. (2) shows that $U_D(k)$ is a first-order, discrete dynamic variable with input I and output U_D , which can be constructed through MATLAB System Identification App. Hence, the primary task is to decompose the measured terminal voltage into two parts: diffusion and non-diffusion components. To this end, we propose an iterative scheme shown in Fig 2.

Figure 4. An Iterative Scheme for Battery Model Identification



Several points about the identification scheme are presented below. First, the input variables, current, and temperature are always measurable. Second, the output variable, OCV, or diffusion voltage should be estimated during the identification. Third, we initially assume the estimated diffusion voltage U_D to be zero in order to obtain the model of U_{OCV} . Then the estimated OCV will enable us to reconstruct the diffusion voltage by building a single-input-single-output (SISO), first-order z-transfer function (z-TF) model:

$$\frac{U_D}{I} = \frac{R_D \left(1 - \exp\left(-\frac{\Delta t}{R_D C_D}\right) \right)}{1 - \exp\left(-\frac{\Delta t}{R_D C_D}\right) z^{-1}} \quad (7)$$

Here the input is the current I , and the estimated diffusion voltage derived by $U_t - \hat{U}_{OCV} + I\hat{R}_I$ is the output for z-TF modeling. Note that we use a single z-TF to model both discharging and charging because the input-output data used in the standard transfer function identification method should be an uninterrupted time series. Fourth, once the z-TF model is obtained, we need to re-estimate the OCV and RI because the diffusion voltage has changed. We repeat this LASSO and z-TF identification procedure iteratively while maintaining a solution pool because the model mean absolute error (MAE) may not be monotonically reduced during the iteration. When a predetermined number of iterations, denoted as N , has been achieved, we screen the pool and choose the model with minimal MAE.

2.2 SOC Estimation

A New Coulomb Model

Coulomb counting is one of the most common methods for SOC estimation based on the current integration. The mathematical formula of this method is:

$$s(k) = s(k-1) - \frac{\eta}{Q} \int_0^{\Delta t} I dt,$$

where Δt is the sampling time interval, Q is the nominal capacity, and η is the Coulomb efficiency. Given the input current and output SOC, the parameter $\frac{\eta}{Q}$ can be identified through the data fitting. However, the sensitivity of the resulting model is the main issue, especially under the low-current scenario. Hence, a new Coulomb model is proposed in this report:

$$s(k) = s(k-1) - \beta_0 |I(k-1)| - \beta_1 I(k-1) - \beta_2 I^2(k-1) - \beta_3 T(k-1) - \beta_4 \quad (9)$$

where $\beta_0, \beta_1, \beta_2, \beta_3, \beta_4$ are model parameters for the SOC change during consecutive time instants. Compared with the modified Coulomb method (Chang, 2013), our model integrates more terms and relies on LASSO to select suitable features in the model. For different batteries, the selected feature set can be adjusted by applying LASSO on the battery test datasets. If the initial SOC is known and the current measurement is accurate, then the Coulomb method is the most convenient way of performing SOC estimation. In the case study, we will show that the proposed new Coulomb model leads to more accurate SOC estimation than the conventional one.

Moving Horizon Estimator for SOC

Different from commonly used filter methods, we employ an optimization-based framework, MHE, to estimate the SOC. MHE minimizes the estimation error of observation over a backward sliding window and moves one step forward at each time instant. The advantages of MHE include the following: (1) automatically determining the initial SOC, (2) fewer parameters to tune, and (3) explicitly handling the non-linearity of the battery model. On the other hand, it needs to solve an optimization problem online, which requires more powerful computational resources than filter-based approaches. To our best knowledge, few works have considered MHE in the battery SOC estimation.

In terms of voltage-based MHE, the SOC can be estimated purely based on the voltage model using MHE, denoted as V-MHE. Note that diffusion voltage usually is significantly smaller than the non-diffusion counterpart, and Eq. (2) is mainly driven by the input current. We can assume $U_D(k_0) = 0$ at the initial time instant k_0 , and the diffusion voltage estimation $\hat{U}_D(k)$ can be derived independently since it only needs the current input I . Then the non-diffusion voltage $U_t(k) - \hat{U}_D(k)$, as the observation, will be used in the MHE to determine SOC. The optimization formula of V-MHE at time instant k is:

$$\sum_{j=0}^H (U_t(k-j) - \widehat{U}_D(k-j) - f^T(k-j|k)^{(\cdot)} \alpha^{(\cdot)})^2 \quad (\text{V-MHE})$$

subject to: Eq. (6)

$$\hat{s}(k-j|k) \geq \hat{s}(k-j-1|k), \text{ if } I(k-j-1) < 0, \quad (10)$$

$$\hat{s}(k-j|k) \geq \hat{s}(k-j-1|k), \text{ if } I(k-j-1) \geq 0, \quad (11)$$

$$\hat{s}(k-j|k) \in [0,1], \forall j \in \{0, 1, 2, \dots, H\}, \quad (12)$$

$$f^T(k-j|k)^{(\cdot)} \alpha^{(\cdot)} + I(k-j)R_I^{(\cdot)} \in [\underline{U}_{OCV}, \underline{U}_{OCV}], \forall j \in \{0, 1, 2, \dots, H\}, \quad (13)$$

where H is the estimation horizon, and $\hat{s}(k-j|k)$ represents the estimated SOC at time instant $k-j$, given the latest measurement at time instant k . The objective function in V-MHE minimizes the squared summation of estimation error along the horizon. The parameters $f^{(\cdot)}$ and $R_I^{(\cdot)}$ are identified using methods in Section 2.1. Here the superscript (\cdot) can be $(+)$ or $(-)$, determined by the current sign. Similarly, Eqs. (10) and (11) are also dependent on the current sign. The SOC should increase when $I(k-j-1) < 0$, representing charging at time instant $k-j-1$. Otherwise, SOC should be reduced during the discharging time interval. The upper and lower bounds on SOC and voltage are enforced in Eq. (12) and (13). Solving V-MHE will generate a sequence of estimated SOC: $\hat{s}(k-H|k), \hat{s}(k-H+1|k), \dots, \hat{s}(k|k)$. Only the last one, $\hat{s}(k|k)$, will be kept as the latest SOC for real-time decisions.

As for voltage-and-current-based MHE, the SOC can be also estimated based on the voltage and current (improved Coulomb) models using MHE, denoted as VC-MHE. The improved Coulomb method utilizes the current to model the change of SOC, but it is unable to identify the initial SOC value. The V-MHE determines SOC to match the observed terminal voltage and is not dependent on the initial SOC. Integrating these two approaches may provide a more accurate estimation. To this end, we redesign the objective function of the MHE:

$$\sum_{j=0}^H (U_t(k-j) - \widehat{U}_D(k-j) - f^T(k-j|k)^{(\cdot)} \alpha^{(\cdot)})^2 + Q_c \sum_{j=1}^H (\hat{s}(k-j+1|k) - s(k-j|k) + \beta_0 |I(k-1)| + \beta_1 I(k-1) + \beta_2 I^2(k-1) + \beta_3 T(k-1) + \beta_4)^2$$

(VC-MHE) subject to: Eqs. (6), (12), (13)

There are two terms in the objective function of VC-MHE. The first term is the same as the objective function of V-MHE, which minimizes the discrepancy between the voltage measurement and value derived from the battery model. The second term minimizes the difference between SOC change derived from the current measurement (9) and its counterpart in the SOC estimation. The weighting parameter Q_c is introduced to balance the influence from the voltage and current approaches. Here the SOC dynamics have already been incorporated into the objective function by following Eq. (9). Hence, we do not enforce Equations (10) and (11) in VC-MHE.

2.3 Simulation Results

In this section, we use the Sanyo 18650 3.7V 2.6Ah battery test data in [3] for modeling and SOC estimation. In the beginning, several constant current constant voltage (CCCV) cycles were run at gradually increasing C-rates, with variable temperature ranging from 21 to 40 degrees Celsius. Then Multistage Constant Current (MCC), Constant Power-Constant Voltage (CP-CV), and Boostcharge cycles were conducted subsequently at various C-rates. Finally, 1C CCCV baseline tests were executed. The sampling time interval is $\Delta t = 0.1$ second. To solve the MHE, we use a nonlinear program (NLP) solver IPOPT within the MATALB OPTI platform.

Battery Modeling and Validation

The entire dataset is divided into two parts: training and validation. The training part is utilized for model development. The validation part is purely used for the model performance evaluation. The pre-determined iteration number is set as $N = 7$. Here the best model among all iterations is selected by minimizing the MAE:

$$n^* = \arg \min_{n \in \{1, 2, \dots, N\}} \frac{\sum_{k=1}^{K_r} |\hat{U}_t^{[n]}(k) - U_t(k)|}{K_r} \quad (14)$$

where K_r is the total data number in the training datasets and is the estimated terminal voltage in n^{th} iteration. In Table 1, we list the MAE on training datasets in all 7 iterations. The model derived in the second iteration yields the best performance and should be adopted. The parameter values on Table 2 show that discharging and charging may have different characteristics. In addition, LASSO does not choose the feature $\log(s)$ for the discharging model. The z-TF identified through MATLAB App is shown in (15); its parameters can be used to derive R_D and C_D in Eq. (2). The model's predicted output and real measurement on the training set are illustrated in Figure 3 for comparison. In addition, we also plot the predicted output and real measurement on the validation set in Figure. 4. Here we can see that the MAE on the validation set is slightly higher than on the training set but is still at a low level.

Table 1. MAE on Training Datasets in Each Iteration and Validation Set

Iterations	MAE
1	0.01079
2	0.01075
3	0.01078
4	0.01083
5	0.01086
6	0.01086
7	0.01087
Validation	0.02060

$$\frac{U_D}{I} = \frac{1.058 \times 10^{-6}}{1 - 0.9968z^{-1}} \quad (15)$$

Table 2. Battery Model Parameters

Parameter index	(+) Discharging	(-) Charging
α_0	2.7133	4.3847
α_1	0.0169	0.0023
α_2	0.0039	-0.5709
α_3	0.0093	0.0027
α_4	0	0.1508
α_5	-0.00001	-0.0006
α_6	-0.0056	0.0044
α_7	-0.2602	0.0135
α_8	0.0242	0.0013
α_9	0.0824	-0.0170
α_{10}	0.3619	0.0048
α_{11}	0.4988	-0.0476
α_{12}	0.2526	0.00005
α_{13}	0.6060	-0.1032
R_I	0.3191	0.0046

Figure 5. The Battery Model Output vs. Measurement on Training Set

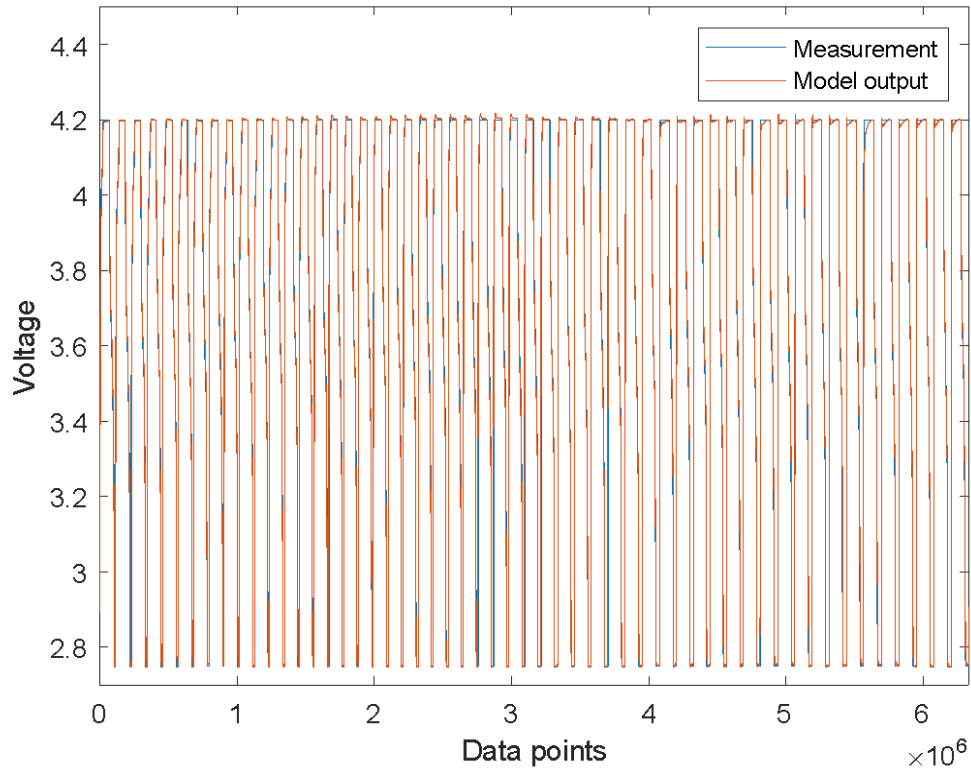


Figure 6. The Battery Model Output vs. Measurement on Validation Set

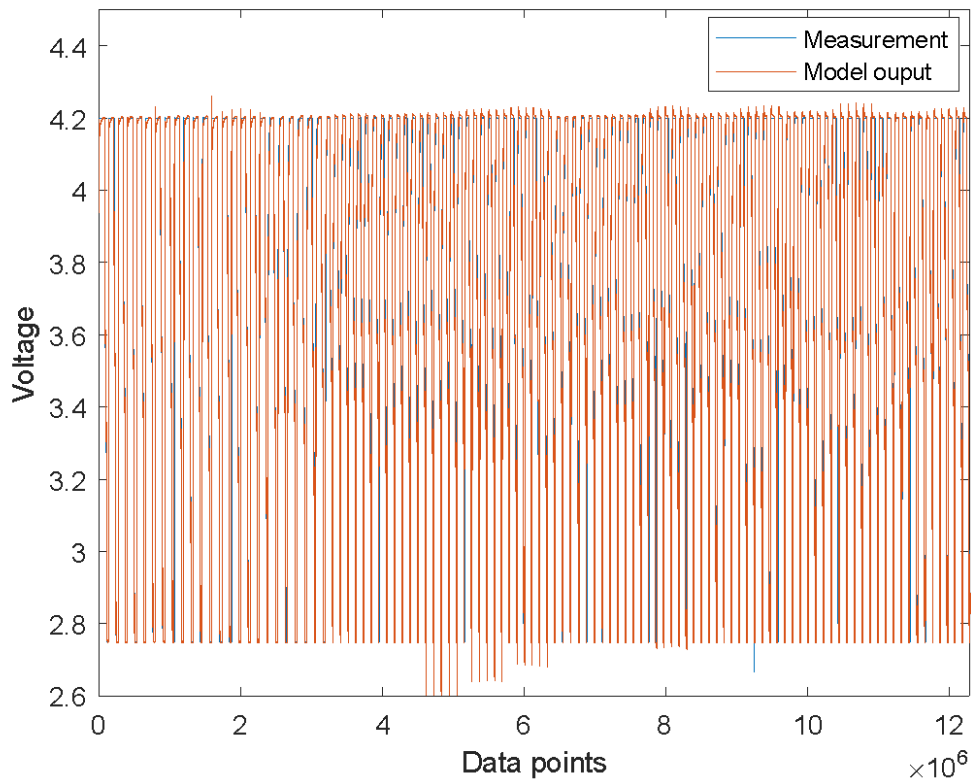
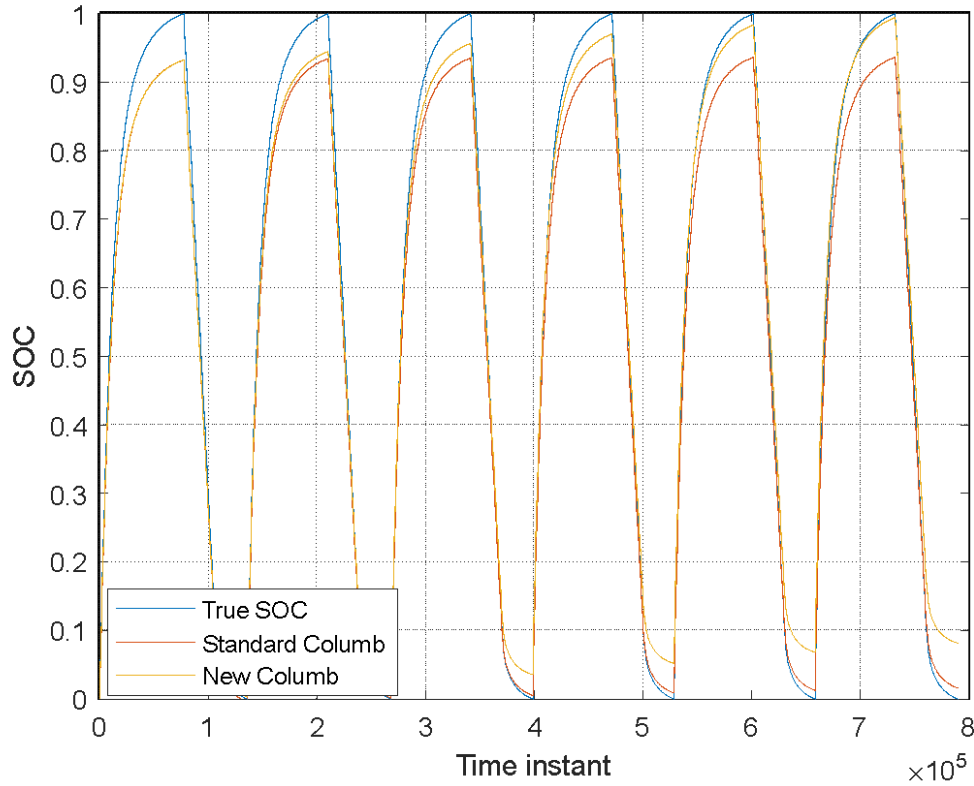


Figure 7. SOC Estimation Based on Coulomb Approaches



SOC Estimation Results

The battery test data also contains the real-time SOC. We use the training dataset to build and compare the standard and new Coulomb models. For the standard Coulomb method, we identify the parameter in Eq. (8) as $\eta = 2.90 \times 10^{-4}$. For the proposed new Coulomb method, Table 3 shows battery model parameters in Eq. (9). In Figure 5, both standard and new Coulomb approaches are applied to estimate the SOC on one of the validation datasets by assuming the zero initial condition. Here we can see that the proposed new model is more accurate at high SOC, whereas the standard Coulomb has better prediction in the low SOC range. However, both methods fail to estimate the initial SOC condition and are less accurate when the charging or discharging current is low. Hence, we use V-MHE or VC-MHE to estimate the initial condition and apply them in a hybrid manner. Once the initial SOC condition is determined by MHE, we may still use it when the current is less than 1 A. Otherwise, the new Coulomb method is applied instead. Due to the intensive computation of the MHE-based algorithm, only a few test points, shown in Table 4, are studied with the weighting parameter $Q_c = 10^4$. The estimated SOC and the true SOC profiles are plotted on Figures 8 and 9 for comparison. Here we can see that during the battery charging process (starting point at 40500), both VC-MHE and V-MHE obtain a similar estimation, which is only a 1% difference from the true SOC. However, V-MHE shows considerably larger fluctuations in the estimated SOC. For the battery discharging process, VC-MHE is far more accurate than the V-MHE approach. As shown in Table 4, VC-MHE is only 0.7% different from the true SOC, whereas the V-MHE has a 27% difference. The reason is that V-MHE is only based on the voltage that has a flat stage when SOC is not significantly high or

low. During that stage, we cannot determine the SOC purely using the terminal voltage measurement.

Table 3. Improved Coulomb Model Parameters

β_0	β_1	β_2	β_3	β_4
-5.04×10^{-7}	1.11×10^{-5}	1.26×10^{-7}	3.85×10^{-8}	-8.59×10^{-7}

Table 4. SOC Estimation Results at Sampled Periods

Starting points	Length	MAE (VC-MHE)	MAE (V-MHE)
40500	500	0.01267	0.01452
99900	500	0.00732	0.27404

Figure 8. SOC Estimation Based on VC-MHE and V-MHE (Starting: 40500)

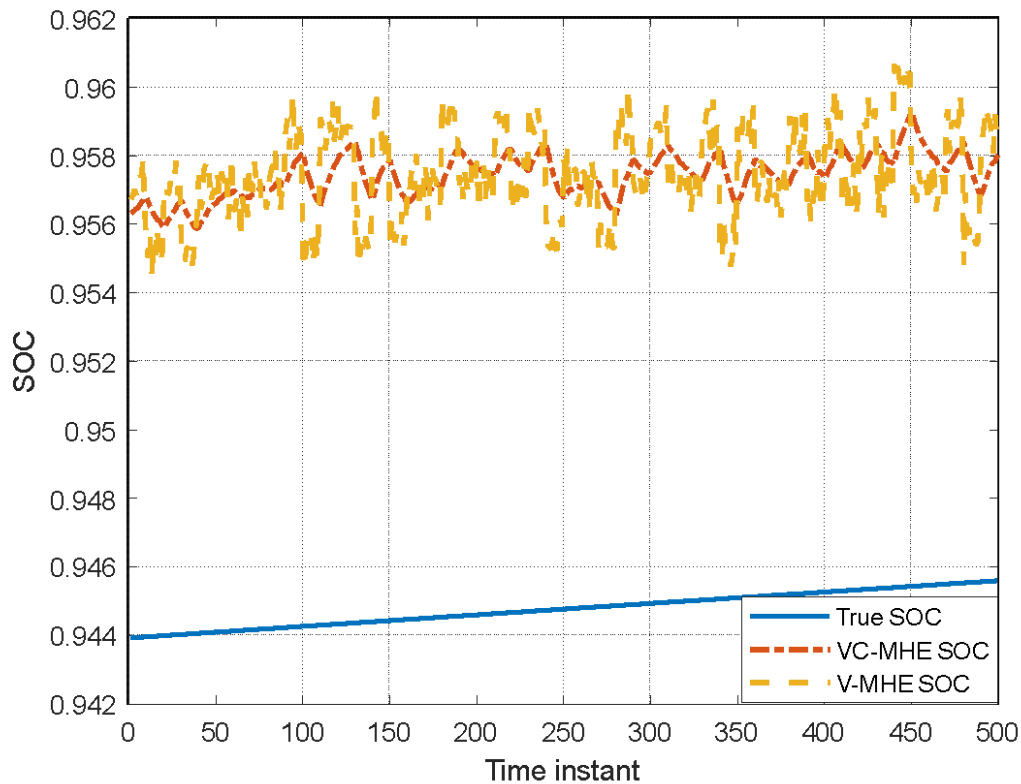
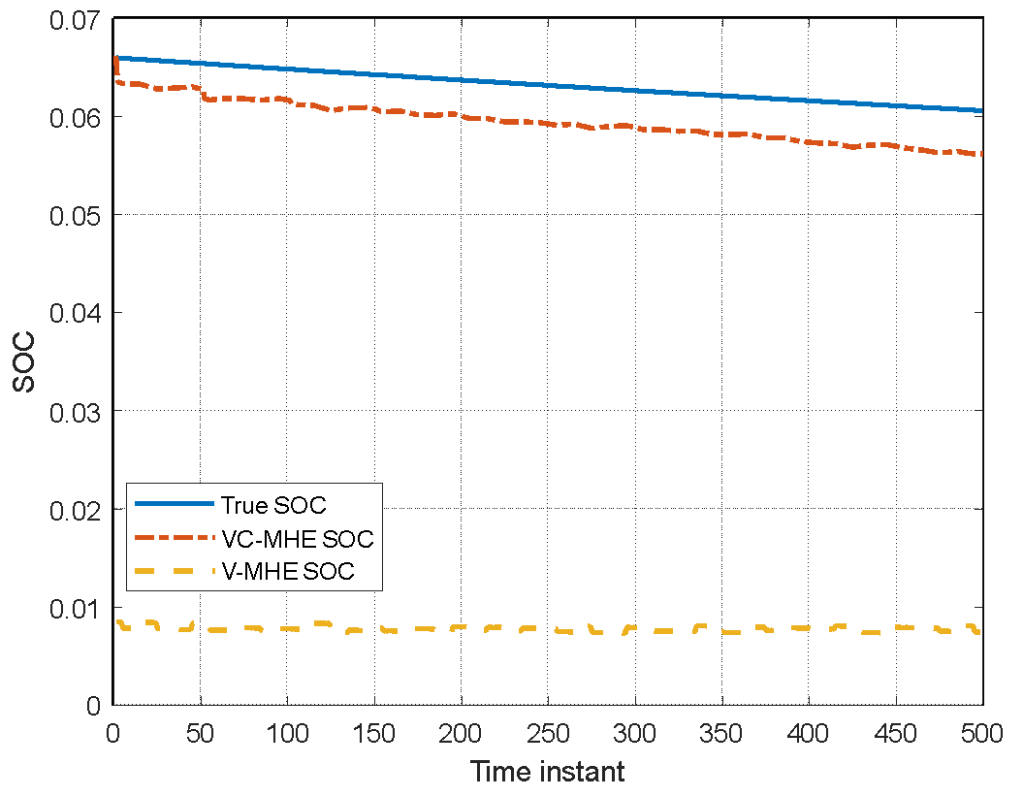


Figure 9. SOC Estimation Based on VC-MHE and V-MHE (Starting: 99900)



3. Field-Programmable Gate Array Implementation

The proposed SOC estimation method is computationally expensive, and thus we consider its FPGA implementation. In this chapter, the primary objective is to validate and execute the SOC estimation method on an FPGA board using MATLAB/SIMULINK. While numerous tutorials and videos are available for the implementation process, adapting them to specific needs can pose challenges. To facilitate understanding, the method is delineated into distinct sections, encompassing equation analysis, MATLAB representation, conversion from floating point to fixed point, FPGA initialization, and the final FPGA implementation.

3.1 Analysis of the Coulomb Counting Equation

SOC estimation is a complex problem that exists in many battery-related applications, depending on multiple parameters and operating conditions. Simultaneously, this complexity is mitigated through the utilization of predefined functions, commonly referred to as “built-in functions.” It is essential to emphasize that transitioning from an equation to a function necessitates a comprehensive understanding of the intended equation and a sound grasp of its underlying theory. Here let us consider a standard Coulomb counting equation for SOC estimation:

$$SOC(k) = SOC(k - 1) + I * 1.21898986449179e^{-5} \quad (16)$$

where k represents the time step and I is the charging/discharging current. Equation (16) is a first-order differential equation. At each step, the SOC is updated by using the current multiplying a constant $1.21898986449179e^{-5}$, which is identified from the dataset discussed in Chapter 2. We will use a technique called “z-transform” to alter the form. By doing this, the z-transform function formula is as follows:

$$SOC(z) = z^{-1}SOC(z) + I(z) * 1.21898986449179e^{-5} \quad (17)$$

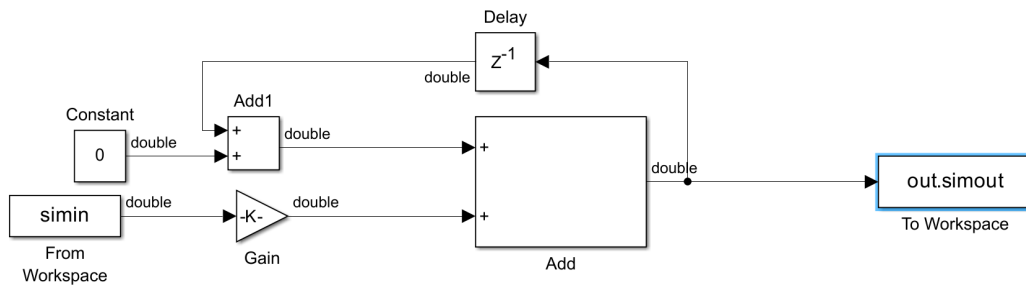
Let us treat SOC as output and I as input values. Then the resulting discrete transfer function model $H(z)$ can be defined in (18).

$$H(z) = \frac{1.218986449179e^{-5}}{(1-z^{-1})} \quad (18)$$

3.2 Implementation on MATLAB/SIMULINK

Before the FPGA implementation, we first deploy this function in MATLAB/SIMULINK. The resulting built-in function is shown in Figure 10.

Figure 10. SIMULINK Build-in Function

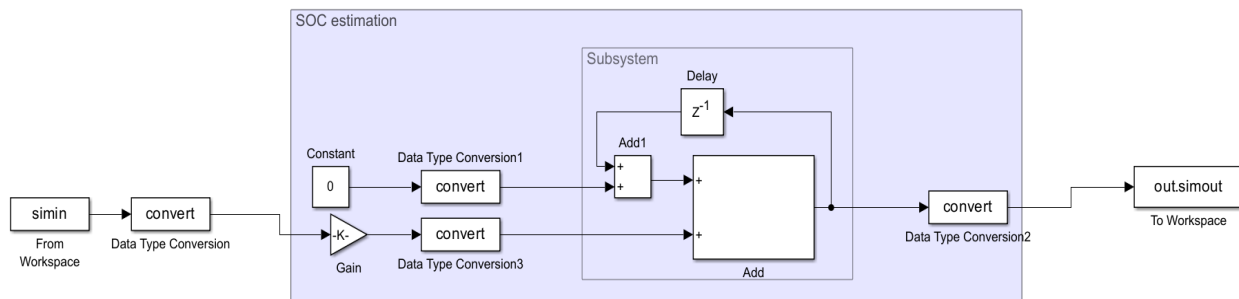


where

- $X(z)$: “From Workspace” is a built-in function block to supply current signal
- $1.218986449179e^{-5}$: “Gain” is a built-in function block to represent the constant value
- $+$: “Add” and “Add1” are the adder built-in function block that combines $X(z)$, $Y(z)$ and $z^{-1}Y(z)$
- 0 : “Constant” is a built-in function block that represents the initial value of SOC
- z^{-1} : “Delay” is a built-in function block
- Out: “To Workspace” is a built-in function block to represent the result.

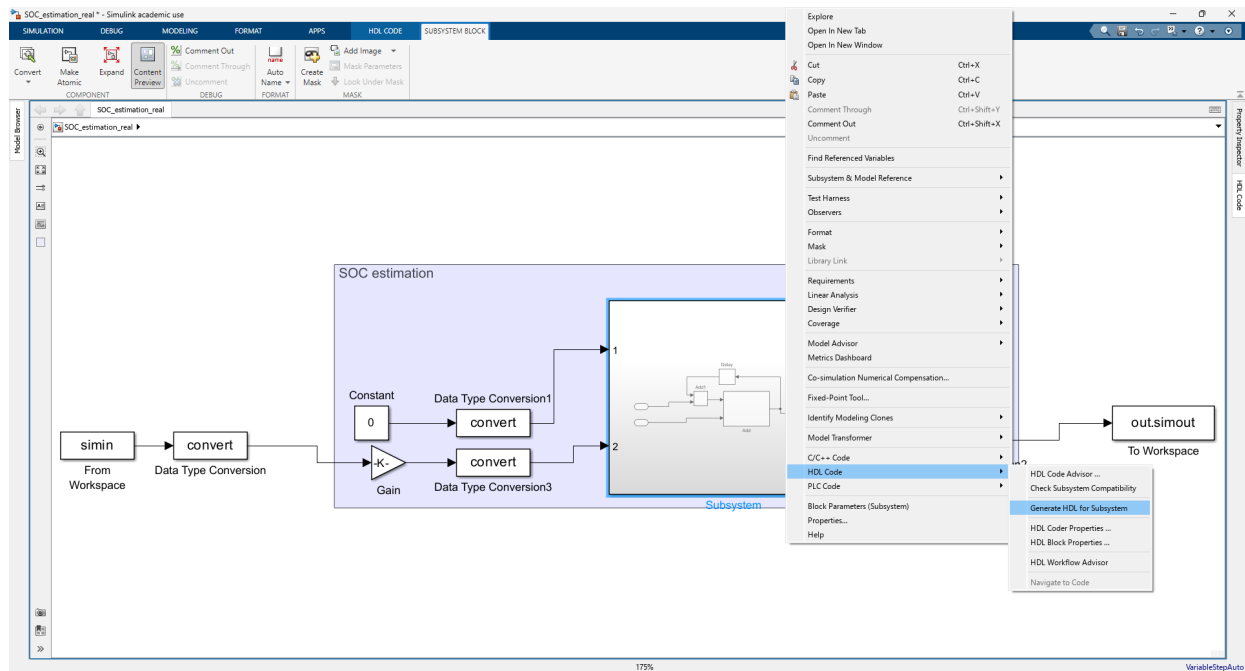
For the goal to implement the Coulomb Counting Equation on a FPGA board, the SIMULINK model must be converted to follow the functionality of the hardware. First, the built-in function blocks should have the sample time of 0.01, matching the real data sampling rate. Next, we create a subsystem called “SOC estimation” with “Convert” blocks, shown in Figure 11.

Figure 11. SIMULINK SOC Subsystem with Convert Blocks



The data type in the convert blocks should be specified by the “fixdt” function. Then we select the SOC estimation subsystem and choose “Create Subsystem from Area” to generate HDL code, as shown in Figure 12. Once completed, the “Command Window” will display the process for MATLAB to create the HDL code. In that history of the process, the location of the file can be shown. It is important to remember where the file is located and to make sure it is saved on the same path that MATLAB is using. The file that will be used is the “Subsystem.vhd.”

Figure 12. SIMULINK HDL Code Generation



3.3 FPGA-in-the-Loop Simulation

For initialization of the FPGA, the FPGA board Basys3 and additional software are utilized. To execute the function on the board, “JTAG” must be applied. This is done manually by changing the “JP1” pin to “JTAG” and having a proper USB cable. The required software(s) are listed below:

- Vivado 2022.1
- MATLAB R2023.b or older
- HDL Coder
- HDL Verifier
- Fixed-point Designer

- HDL Coder Support Package for Xilinx FPGA Boards
- HDL Verifier Support Package for Xilinx FPGA Boards

The built-in command “hdlsetuptoolpath” on MATLAB enables Vivado and MATLAB to communicate:

```
hdlsetuptoolpath('ToolName','Xilinx
Vivado','ToolPath','C:\Xilinx\Vivado\2022.1\bin\vivado.bat').
```

Here the path shows where the Vivado is located in the computer. Next, we initialize the FPGA board to MATLAB by executing the built-in command called “filWizard.” This should open an “FPGA-in-the-Loop Wizard” window. Here we need to make sure that the following conditions are fulfilled:

- “FIL simulation with” is on “Simulink”
- “FPGA-in-the-loop connection” is on “JTAG”
- “Advanced Options” is on “FPGA system clock frequency (MHz) to 25”

Because MATLAB does not have the Basy3 in their “FPGA Board List,” we have to add the board manually. To this end, we select “Launch Board Manager” in the “Board Options” section and then go to “Create Custom Board.” This will open the “New FPGA Board Wizard” window. The following information shown in Figures 13 and 14 is filled to add Basy3 board.

Figure 13. Introduce Board Name: Basy3

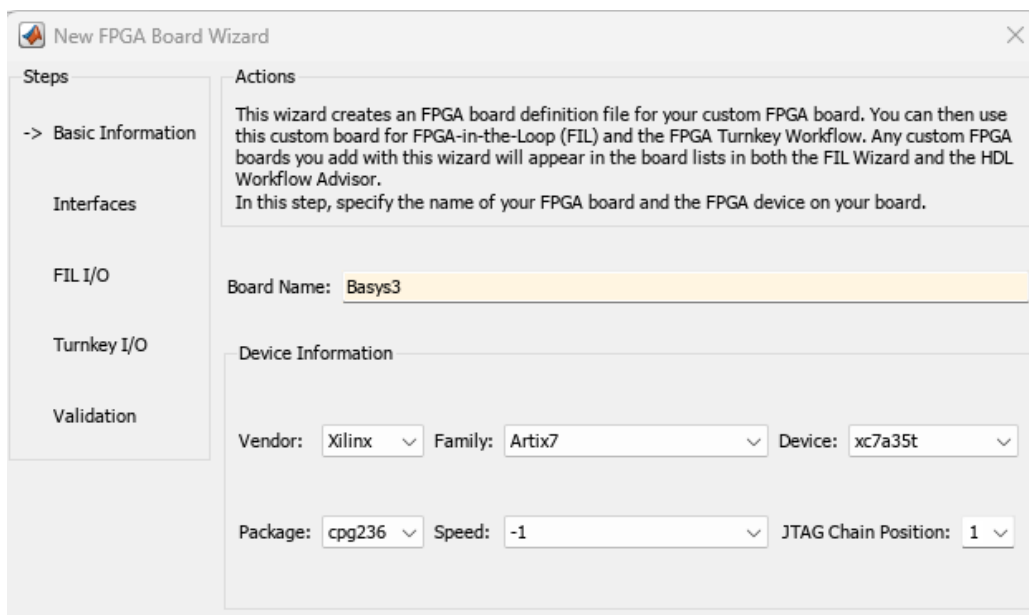
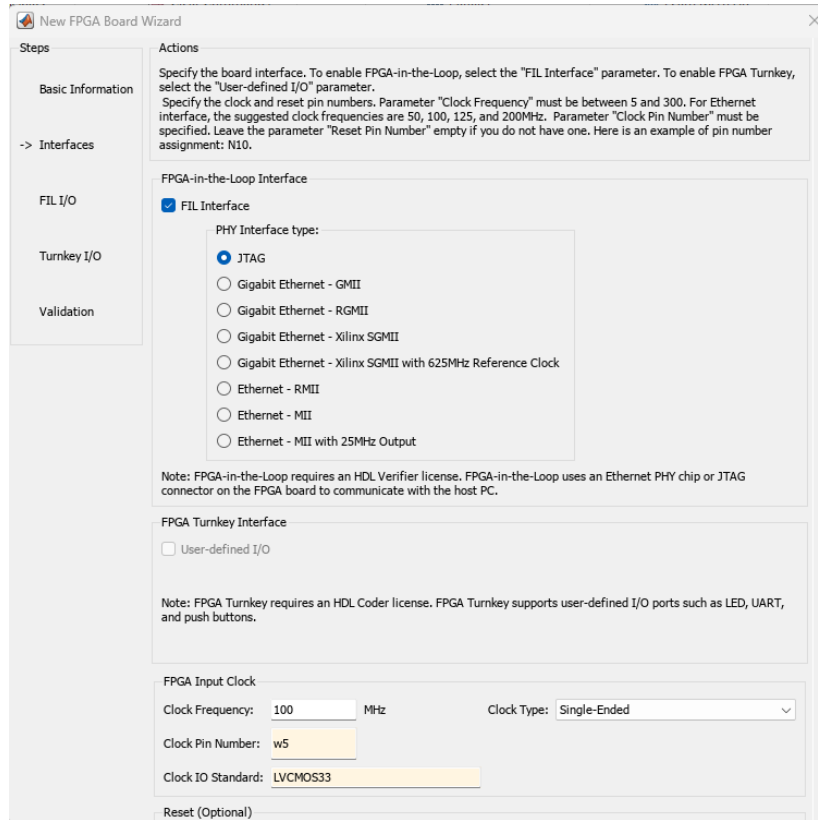


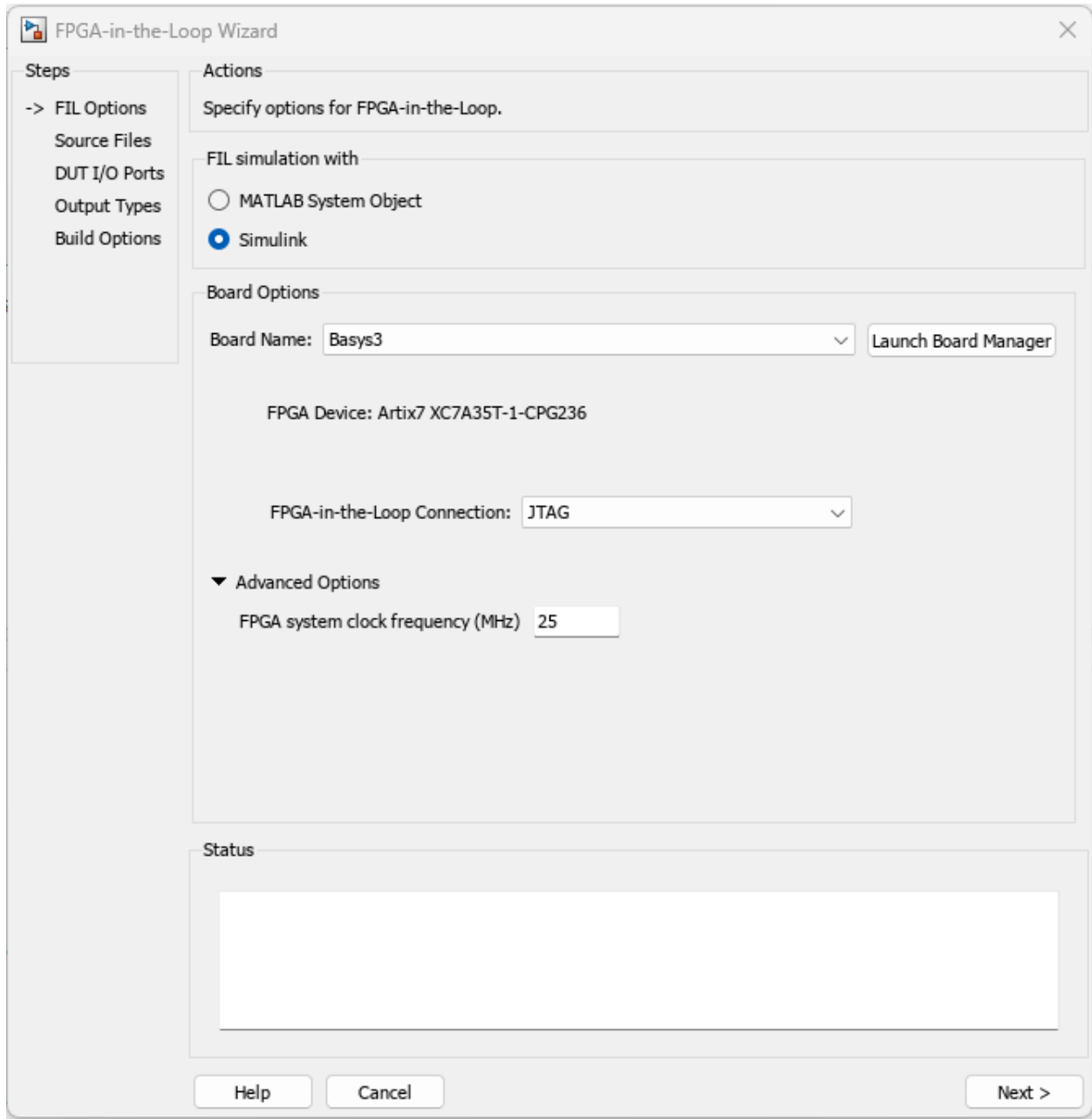
Figure 14. FPGA-in-the-Loop Interface



Note that if errors occur, the help documentation is a powerful tool to address the issue. Sometimes the error could be due to the absence of a license for Vivado or a USB port mismatch. If each step goes well, we should save the file (Basys3.xml) in a folder that is part of the path of the MATLAB file. Then we should be able to view the Basys3 board on “FPGA Board Manager.”

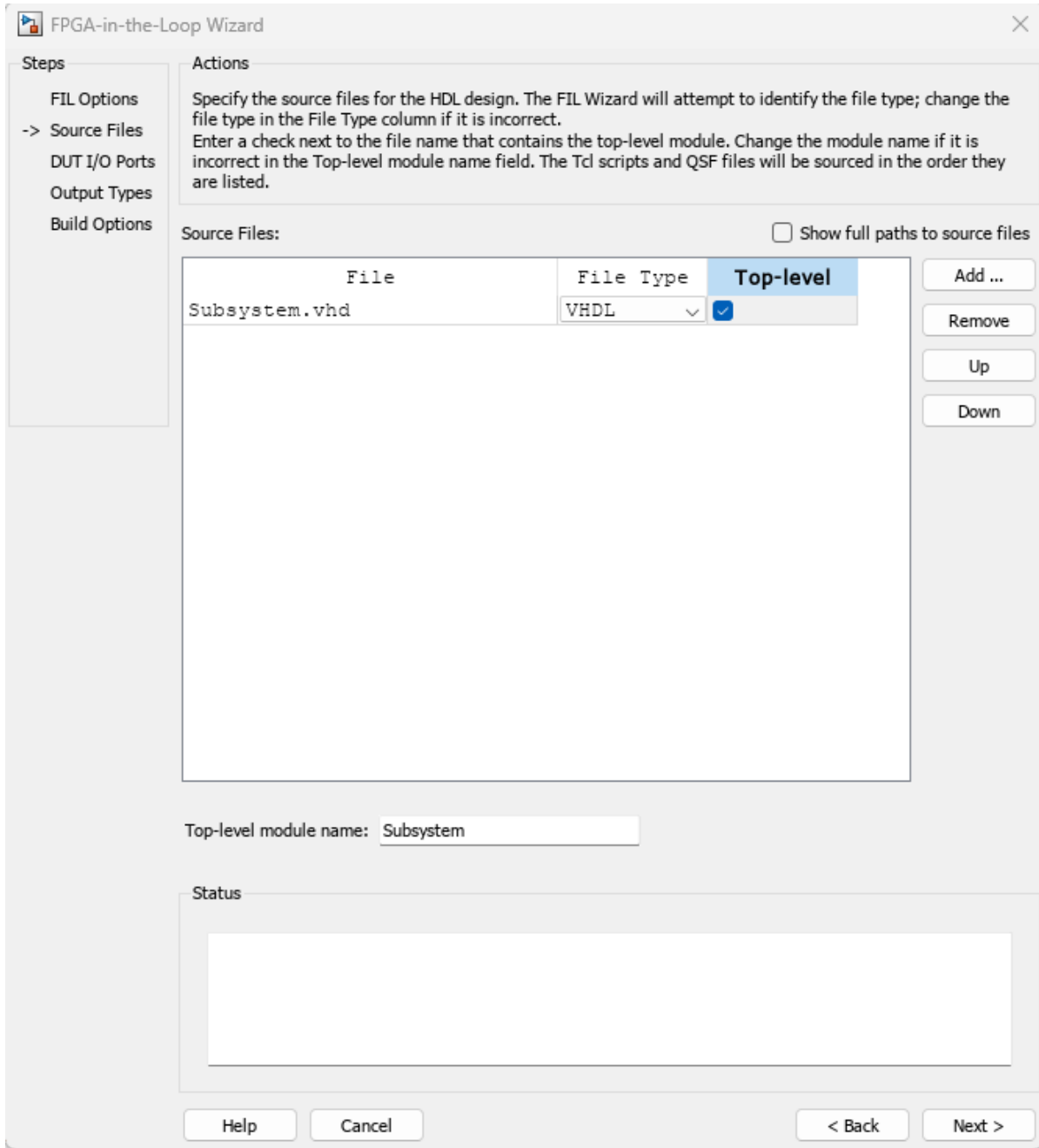
The FPGA-in-the-Loop wizard leads us to embed FPGA with our SIMULINK file. The Basys3 board is selected, and the connector is JTAG, as shown in Figure 15.

Figure 15. FPGA-in-the-Loop (FIL) Options



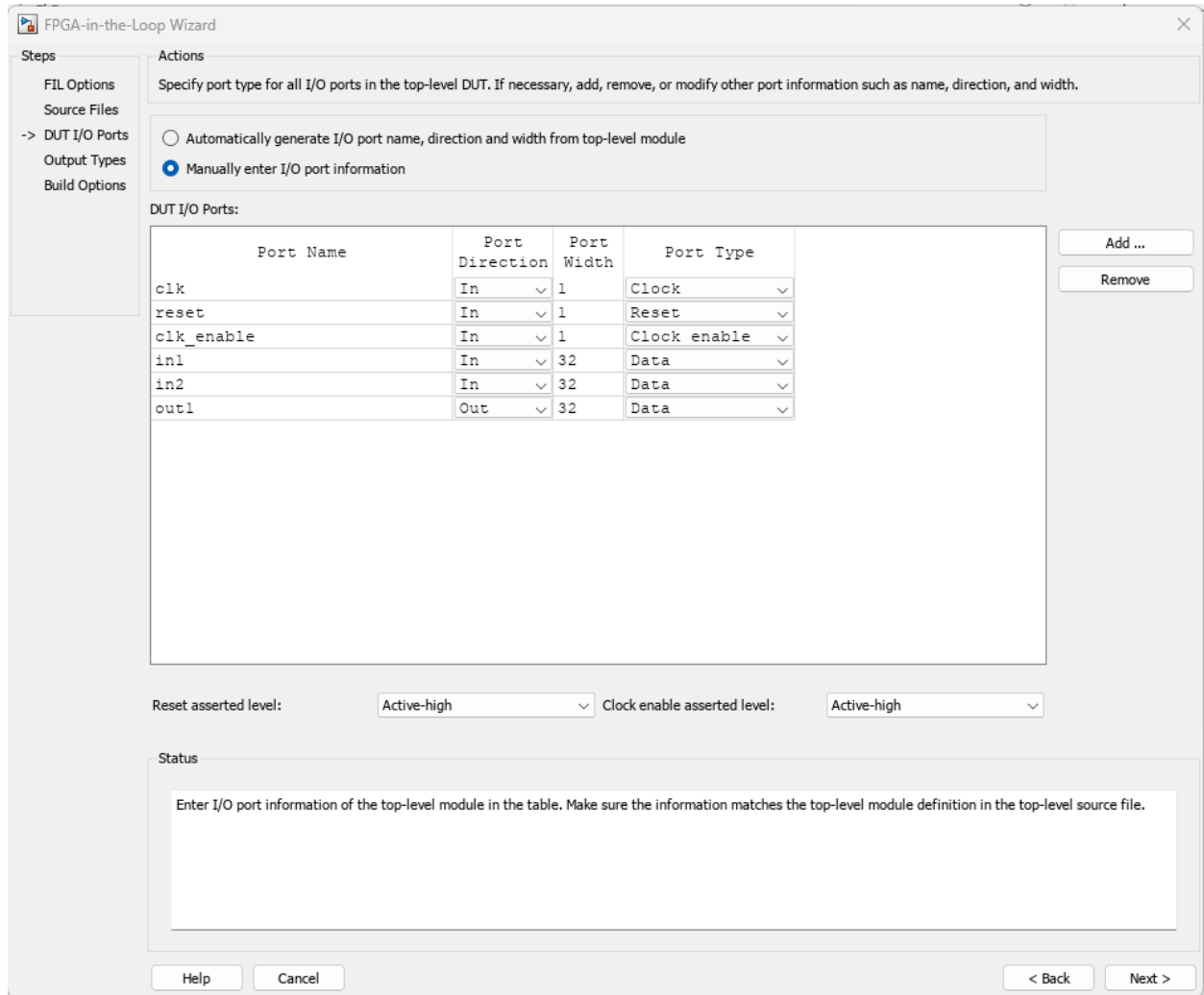
The source files shown in the top left corner of the wizard should be the “Subsystem.vhd.” Recall the location of the file and add the file. Then make sure to mark “Top-level,” as in Figure 16.

Figure 16. FPGA-in-the-Loop (Source Files)



In the next window “DUT I/O Ports,” we manually change the ports by selecting “Manually enter I/O port information,” select “ce_out,” and click “remove,” as shown in Figure 17.

Figure 17. FPGA-in-the-Loop (DUT I/O Ports)

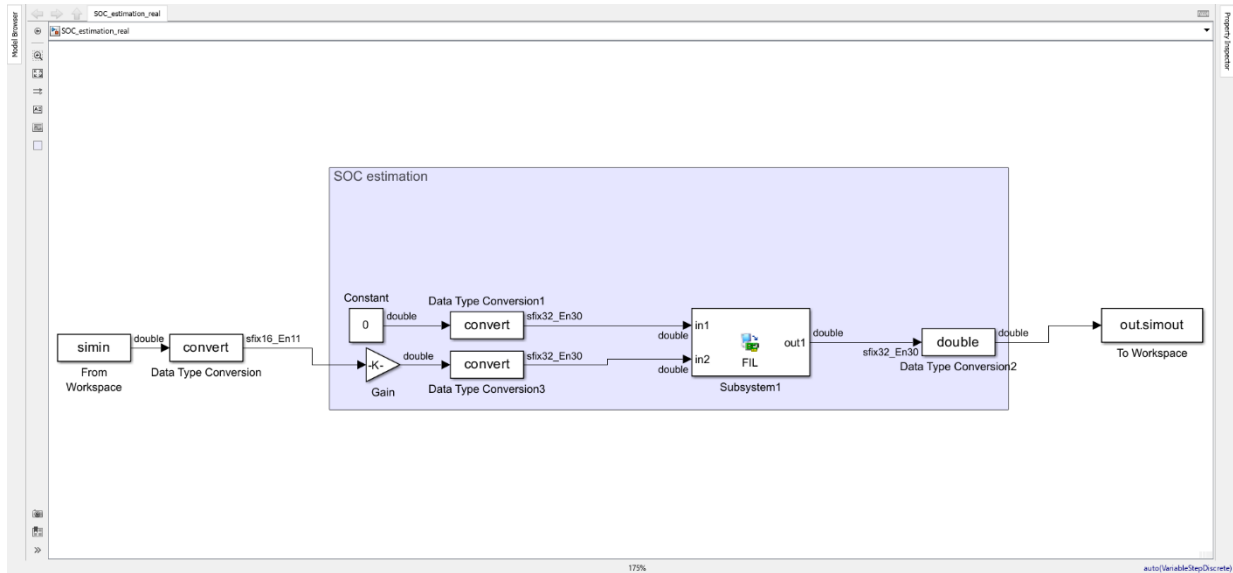


In next window, “Output Types,” the following parameters are required:

- “Bit Width” is 32
- “Data Type” is “Fixedpoint”
- “Sign” is “Signed”
- “Fraction Length” is 30

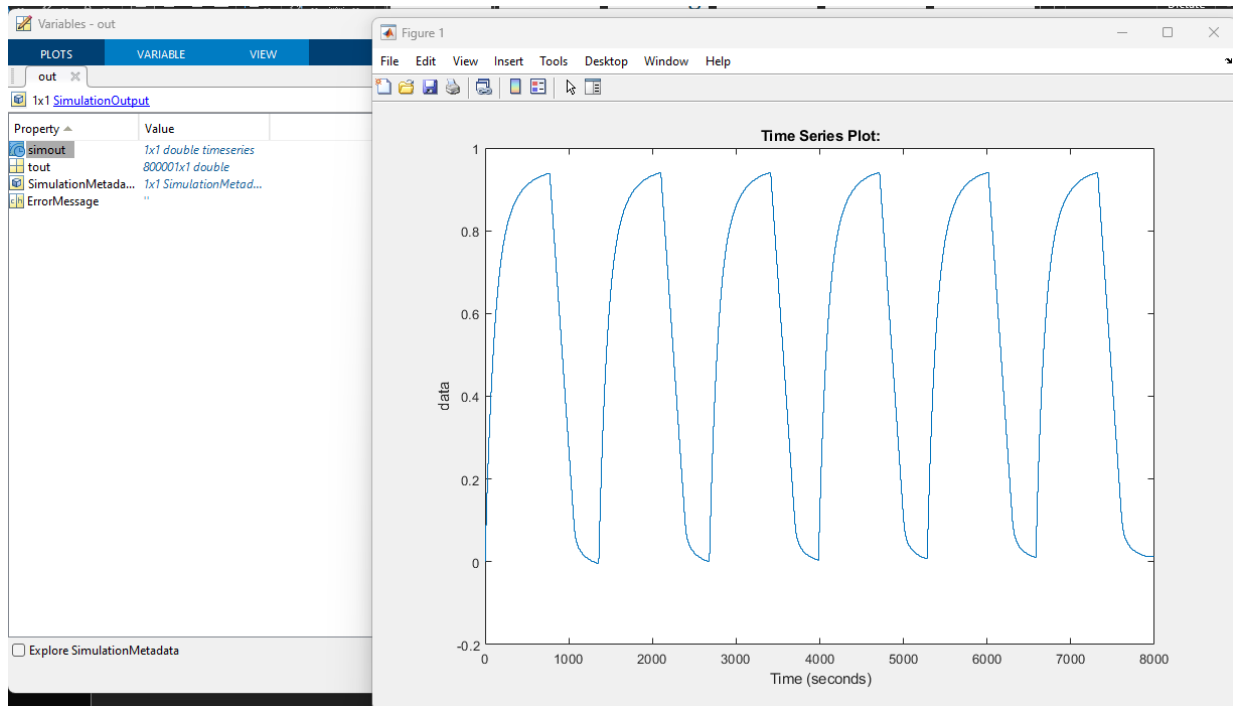
The option “Build Options” allows us to determine the location of the file. If the file is left in the current location, MATLAB will ask to overwrite the existing file. After clicking “Build,” it will generate a process to construct a special built-in function block. This built-in function is where MATLAB will perform the functions on the FPGA. The next step is to remove and delete “subsystem” in the original SIMULINK and modify it with the generated FIL block “Subsystem1,” as show in Figure 18.

Figure 18. Reconstruct SOC Estimation Block with FIL



Then we open the “Subsystem1” and load the FPGA bitstream. Finally, the model is ready to be simulated. Note that the stop time should be set to 8000 to match total data length. The resulting SOC estimation is shown in Figure 19.

Figure 19. SOC Estimation Results via FIL



4. Summary & Conclusions

In this project, the research team proposes a new SOC estimation methodology for lithium-ion batteries, based on an open-source test dataset with a one-battery model. The proposed modeling scheme first develops a new static ECM by using a data analysis technique called LASSO to select important features. Secondly, the dynamic component of the ECM is modeled as a discrete, first-order transfer function. By repeatedly applying LASSO and transfer function identification, the data fitting error is minimized. Once we have the ECM model, we integrate it with the Coulomb counting method within both voltage-based MHE (V-MHE) and voltage-and-current-based MHE (VC-MHE) frameworks. Through simulations, we compare these two schemes and conclude that the VC-MHE is superior to V-MHE because the estimation error can be reduced significantly. The research team also implements the basic Coulomb counting method on an FPGA board within the MATLAB/SIMULINK platform to demonstrate a real-time, hardware-in-the-loop simulation for battery management system (BMS) development. The discoveries in this project can be applied in electric vehicles for battery maintenance and fast charging.

Glossary

BMS	Battery management system
CCCV	Constant current constant voltage
CP-CV	Constant Power-Constant Voltage
DAE	Differential algebraic equations
ECM	Equivalent circuit method
EV	Electric vehicle
FIL	FPGA-in-the-loop
FPGA	Field-programmable gate array
GP	Gaussian Process
HDL	Hardware description language
JTAG	Joint test action group
LASSO	Least absolute shrinkage and selection operator
Li-Ion	Lithium-ion
MAE	Mean absolute error
MCC	Multistage constant current
MHE	Moving horizon estimator
NCA	Lithium nickel cobalt aluminum oxides
NLP	Nonlinear program
NN	Neural network
OCV	Open circuit voltage
P2D	Pseudo-2-dimensional

PDE	Partial differential equation
POD	Proper orthogonal decomposition
RC	Resistor-capacitor
RMSE	Root Mean Square Error
SOC	State of charge
SOH	State of health
UKF	Unscented Kalman filtering
V-MHE	Voltage-based MHE
VC-MHE	Voltage-and-current-based moving horizon estimator
ZEV	Zero-emission vehicle

Bibliography

- Alexander, A., Crisostomo, N., Krell, W., Lu, J., and Ramesh, R. “Assembly Bill 2127 Electric Vehicle Charging Infrastructure Assessment (Revised Staff Report),” California Energy Commission, 2021.
- Berecibar, M., Gandiaga, I., Villarreal, I., et al. “Critical review of state of health estimation methods of li-ion batteries for real applications,” *Renew Sustain Energy Rev*, 56 (2016): 572–587.
- Cai, L. and White, R. E. “Reduction of model order based on proper orthogonal decomposition for lithium-ion battery simulations,” *Journal of The Electrochemical Society*, 156 (2009): A154–A161.
- Chang, W. Y. The state of charge estimation methods for battery: A review. *ISRN Applied Mathematics*, (2013): 953792
- Chen, Y., Liu, X., Fathy, H. K., Zou, J., and Yang, S. “A graph-theoretic framework for analyzing the speeds and efficiencies of battery pack equalization circuits,” *Int. J. Electr. Power Energy Syst.*, 98 (2018): 85–99.
- Dao, T., Vyasarayani, C. P., and McPhee, J. “Simplification and order reduction of lithium-ion battery model based on porous-electrode theory,” *Journal of Power Sources*, 198 (2012): 329–337.
- Dong, G., Zhang, X., Zhang, C., et al. “A method for state of energy estimation of lithium-ion batteries based on neural network model,” *Energy*, 90 (2015): 879– 88.
- Duraisamy, T. and Kaliyaperumal, D. “Machine learning-based optimal cell balancing mechanism for electric vehicle battery management system,” *IEEE Access*, 9 (2021): 132846–132861.
- Etxandi-Santolaya, M., Casals, L. C., and Corchero, C. “Extending the electric vehicle battery first life: Performance beyond the current end of life threshold,” *Helvion*, 10 (2024): e26066.
- Gandolfo, D., Brandão, A., Patiño, D., and Molina, M. “Dynamic model of lithium polymer battery- load resistor method for electric parameters identification,” *J. Energy Inst.* , 88 (2015): 470–479.
- Gun, D., Perez, H., Moura, S. “Fast Charging Tests,” Dryad, Dataset (2015), <https://doi.org/10.6078/D1MS3X>.

- He, Y., Liu, X., Zhang, C., and Chen, Z. “A new model for State-of-Charge (SOC) estimation for high-power Li-ion batteries,” *Applied Energy*, 101 (2013): 808–814.
- Kumar, B., Khare, N., and Chaturvedi, P. K. “FPGA-based design of advanced BMS implementing SoC/SoH estimators,” *Microelectronics Reliability*, 84 (2018): 66–74.
- Liu, K., Li, K., Peng, Q., and Zhang, C. “A brief review on key technologies in the battery management system of electric vehicles,” *Frontier of Mechanical Engineering*, 14 (2019): 47–64.
- Liaw, B.Y., Nagasubramanian, G., Jungst, R. G. and Doughty, D. H. “Modeling of lithium ion cells—A simple equivalent-circuit model approach,” *Solid State Ionics*, 175 (2004): 835–839.
- Omariba, Z. B., Zhang, L., and Sun, D. “Review of battery cell balancing methodologies for optimizing battery pack performance in electric vehicles,” *IEEE Access*, 7 (2019): 129335–129352.
- Plett, G. L. “Extended Kalman filtering for battery management systems of LiPB-based HEV battery packs Part 2. Modeling and identification,” *Journal of Power Source*, 134 (2004): 262– 276.
- Richardson, R. R., Osborne, M. A., and Howey, D. A. “Gaussian process regression for forecasting battery state of health,” *Journal of Power Sources*, 357 (2017): 209–219.
- Sahinoglu, G. et al, “Battery state-of-charge estimation based on regular recurrent Gaussian process regression,” *IEEE Trans. Ind. Electron*, 65 (2017): 4311–4321.
- Ng, K. S., Moo, C., Chen, Y., and Hsieh, Y. “Enhanced coulomb counting method for estimating state-of-charge and state-of-health of lithium-ion batteries,” *Applied Energy*, 86 (2009): 1506– 1511.
- Smith, K. A., Rahn, C. D., and Wang, C. “Control oriented 1D electrochemical model of lithiumion battery,” *Energy Conversion and Management*, 48 (2007): 2565– 2578.
- Smith, K. A., Rahn, C. D., and Wang, C. “Model-Based electrochemical estimation and constraint management for pulse operation of lithiumion batteries,” *IEEE Transactions on Control System Technology*, 18 (2010): 654–663.
- Sun, F., Hu, X., Zou, Y., and Li, S. “Adaptive unscented Kalman filtering for state of charge estimation of a lithium-ion battery for electric vehicles,” *Energy*, 36 (2011): 3531–3540.

- Wang, Q. K., He, Y. J., Shen, J. N., et al. “A unified modeling framework for lithium-ion batteries: an artificial neural network based thermal coupled equivalent circuit model approach,” *Energy*, 138 (2017): 118–132.
- The White House, FACT SHEET: FACT SHEET: Biden-Harris Administration Driving U.S. Battery Manufacturing and Good-Paying Jobs <https://www.whitehouse.gov/briefing-room/statements-releases/2022/10/19/fact-sheet-biden-harris-administration-driving-u-s-battery-manufacturing-and-good-paying-jobs> Retrieved at Oct 30, 2022.
- Widanage, W. D. et al. “Design and use of multisine signals for Li-ion battery equivalent circuit modelling. Part 2: Model estimation,” *Journal of Power Sources*, 324 (2016): 61–69,
- Yang, D., Wang, Y., Pan, R., Chen, R., and Chen, Z. “A neural network based state-of-health estimation of lithium-ion battery in electric vehicles,” *Energy Procedia*, 105 (2017): 2059–2064.
- Yatsui, M. W. and Bai, H. “Kalman filter based state-of-charge estimation for lithium-ion batteries in hybrid electric vehicles using pulse charging,” *Proceedings of the 7th IEEE Vehicle Power and Propulsion Conference (VPPC '11)*, pp. 1–5, Chicago, IL, USA, 2011.

About the Authors

Yu Yang, PhD

Dr. Yang received his BSc degree from Beijing Institute of Technology, Beijing, China, in 2004; his MSc degree from Zhejiang University, Hangzhou, China, in 2007; and his PhD from the Department of Chemical Engineering, University of Alberta, Edmonton, Canada, in 2011. He then became a postdoctoral associate at the Massachusetts Institute of Technology. He currently is an associate professor in the Department of Chemical Engineering at California State University, Long Beach. His research interests include data-driven modeling, advanced process control, machine learning, global optimization under uncertainty, and the analysis and design of renewable energy systems.

Hen-Geul Yeh, PhD

Dr. Yeh received his BSc degree in engineering science from National Chen Kung University, Taiwan, ROC in 1978; his MSc in mechanical engineering from the University of California, Irvine in 1979; and PhD in electrical engineering, also from the University of California, Irvine in 1982. Since 1983, he has been with the Electrical Engineering Department at CSULB and has served as the Department Chair from 2016 to 2022. In addition to his technical and engineering excellence, he was selected as a NASA JPL Summer Faculty Fellow in both 1992 and 2003 and the Boeing Welliver Faculty Fellow in 2006. His research interests include DSP/Communication/Control algorithms development using MATLAB and their implementation using FPGA. He is also interested in digital signal processors with applications in communication systems, smart grids, optimization, controls, and electrical event detection, with a focus on real-time digital signal processing, Wi-Fi and Wi-MAX, adaptive systems, and mobile communication in multipath fading channels. He has published over 100 research papers on signal processing, communications, controls, and smart grids.

Cesar Ortiz

Cesar Ortiz transferred to California State University, Long Beach in the fall of 2017 to pursue a bachelor's degree in electrical engineering and sought a hiatus to embed himself in the labor industry in 2019. In the spring of 2022, Cesar returned to his studies with a revitalized perspective. Currently, under the guidance of Dr. Yu Yang and Dr. Hen-Guel Yeh, Cesar is working with Digital Signal Processing (DSP) and its applications using MATLAB, Simulink, and FPGA. His research interests include DSP/Communication/Control algorithms development using MATLAB.

MTI FOUNDER

Hon. Norman Y. Mineta

MTI BOARD OF TRUSTEES

Founder, Honorable Norman Mineta***
Secretary (ret.),
US Department of Transportation

Chair, Jeff Morales
Managing Principal
InfraStrategies, LLC

Vice Chair, Donna DeMartino
Retired Transportation Executive

Executive Director, Karen Philbrick, PhD*
Mineta Transportation Institute
San José State University

Rashidi Barnes
CEO
Tri Delta Transit

David Castagnetti
Partner
Dentons Global Advisors

Maria Cino
Vice President
America & U.S. Government
Relations Hewlett-Packard Enterprise

Grace Crunican**
Owner
Crunican LLC

John Flaherty
Senior Fellow
Silicon Valley American
Leadership Form

Stephen J. Gardner*
President & CEO
Amtrak

Ian Jefferies*
President & CEO
Association of American Railroads

Diane Woodend Jones
Principal & Chair of Board
Lea + Elliott, Inc.

Priya Kannan, PhD*
Dean
Lucas College and
Graduate School of Business
San José State University

Will Kempton**
Retired Transportation Executive

David S. Kim
Senior Vice President
Principal, National Transportation
Policy and Multimodal Strategy
WSP

Therese McMillan
Retired Executive Director
Metropolitan Transportation
Commission (MTC)

Abbas Mohaddes
CEO
Econolite Group Inc.

Stephen Morrissey
Vice President – Regulatory and
Policy
United Airlines

Toks Omishakin*
Secretary
California State Transportation
Agency (CALSTA)

April Rai
President & CEO
Conference of Minority
Transportation Officials (COMTO)

Greg Regan*
President
Transportation Trades Department,
AFL-CIO

Rodney Slater
Partner
Squire Patton Boggs

Paul Skoutelas*
President & CEO
American Public Transportation
Association (APTA)

Kimberly Slaughter
CEO
Systra USA

Tony Tavares*
Director
California Department of
Transportation (Caltrans)

Jim Tymon*
Executive Director
American Association of
State Highway and Transportation
Officials (AASHTO)

Josue Vaglienty
Senior Program Manager
Orange County Transportation
Authority (OCTA)

* = Ex-Officio
** = Past Chair, Board of Trustees
*** = Deceased

Directors

Karen Philbrick, PhD
Executive Director

Hilary Nixon, PhD
Deputy Executive Director

Asha Weinstein Agrawal, PhD
Education Director
National Transportation Finance
Center Director

Brian Michael Jenkins
National Transportation Security
Center Director

